

## Oxidative Degradation of Ethers Promoted by Strontium and Barium Tetraphenylimidodiphosphinates

Jesús Morales-Juárez, Raymundo Cea-Olivares,\* Mónica M. Moya-Cabrera, Vojtech Jancik, Verónica García-Montalvo, and Rubén A. Toscano

Instituto de Química, UNAM, Circuito Exterior, Ciudad Universitaria, 04510 México D.F., México

Received May 9, 2005

The novel  $M[(OPPh_2)_2N]_2 \cdot nTHF$  ( $M = Sr$  (**2**),  $Ba$  (**3**)) complexes were prepared and characterized. Upon exposure to atmospheric oxygen, **2** and **3** were transformed to the dinuclear species  $Sr_2[(OPPh_2)_2N]_4 \cdot 2C_3H_6O_3$  (**4**) and  $Ba_2[(OPPh_2)_2N]_4 \cdot 2C_4H_8O_3$  (**5**), respectively. Compounds **4** and **5** contain coordinated carboxylic acids obtained from the oxidative degradation of DME and THF, respectively, which were used as solvents for crystallization.

Transition-metal oxides in high oxidation states are known to be stoichiometric oxidation agents for ethers capable of oxidizing them to the corresponding carboxylic acids, esters, or lactones.<sup>1,2</sup> Thus, attempts have been made to develop such types of oxidizing agents with catalytic behavior. Transition-metal complexes such as  $CoCl_2$ ,  $Co(acac)_3$ ,<sup>3,4</sup>  $RuCl_2[(CH_3)_2SO]_4$ , and  $[Pd(P^tBu_2H)(\mu-P^tBu_2)]_2$ <sup>5,6</sup> have proven to be active in the aerobic oxidation of cyclic and acyclic ethers to lactones, where this process is catalytic in the case of Ru and Pd. Moreover, Rh and Ir complexes catalyze the oxidation of THF to  $\gamma$ -butyrolactone in the presence of small amounts of water.<sup>7</sup> Additionally, the bimetallic complexes  $Ind(CO)_3Mo-Ru(CO)_2Cp$  and  $Fe_2(\mu-O_2CAr^{tO})_2(Me_2TACN)_2-(MeCN)_2(OTf)_2$  have been used to promote the catalytic oxidation of THF.<sup>8,9</sup>

Recently, we have reported on a calcium tetraphenylimidodiphosphinate complex containing coordinated  $\alpha$ -hydroperoxytetrahydrofuran molecules formed by in situ oxidation

of the solvating THF.<sup>10</sup> Because hydroperoxides are known intermediates in the oxidative ring opening of THF, we decided to study the oxidation abilities of tetraphenylimidodiphosphinate complexes based on the heavier alkaline-earth metals, strontium and barium, toward cyclic and acyclic ethers. Herein, we describe the synthesis and characterization of  $Sr[(OPPh_2)_2N]_2 \cdot 2.8THF$  (**2**) and  $Ba[(OPPh_2)_2N]_2 \cdot 3THF$  (**3**), along with the crystal structures of the dinuclear species  $Sr_2[(OPPh_2)_2N]_4 \cdot 2C_3H_6O_3$  (**4**) and  $Ba_2[(OPPh_2)_2N]_4 \cdot 2C_4H_8O_3$  (**5**). Compounds **4** and **5** contain carboxylic acids obtained by the aerobic oxidative degradation of DME and THF, respectively. To our knowledge, this is the first case where main-group metals proved to be active in an oxidative degradation of ethers.

**2** was obtained in high yield (94%) by bubbling dry  $NH_3$  through a suspension of tetraphenylimidodiphosphinic acid (**1**) and activated Sr in THF,<sup>11</sup> whereas the reaction of  $BaCl_2 \cdot 2H_2O$  with  $K[(OPPh_2)_2N]$  in THF led to the formation of  $Ba[(OPPh_2)_2N]_2 \cdot 3THF$  (**3**) in 85% yield.<sup>12</sup> Compounds **2** and **3** are white powders sparingly soluble in  $CH_2Cl_2$  and  $CHCl_3$  but insoluble in most organic solvents. Their  $^1H$  NMR spectra display the characteristic signals corresponding to the phenyl groups at  $\delta$  7.2–7.8 ppm along with the characteristic signals for THF ( $\delta$  3.88 and 1.78 ppm for **2** and  $\delta$  3.70 and 1.67 ppm for **3**). The  $^{31}P$  NMR spectra show singlets at  $\delta$  17.6 and 17.7 ppm for **2** and **3**, respectively. The IR spectra of **2** and **3** exhibit strong absorption bands at 1260 and 1262  $cm^{-1}$ , respectively, corresponding to the  $\nu_{as}(P_2N)$  stretching. The MS-FAB<sup>+</sup> of **2** and **3** reveals peaks at  $m/z$  921 and 971, respectively, corresponding to the  $[M[(OPPh_2)_2N]_2]^+$  fragments.

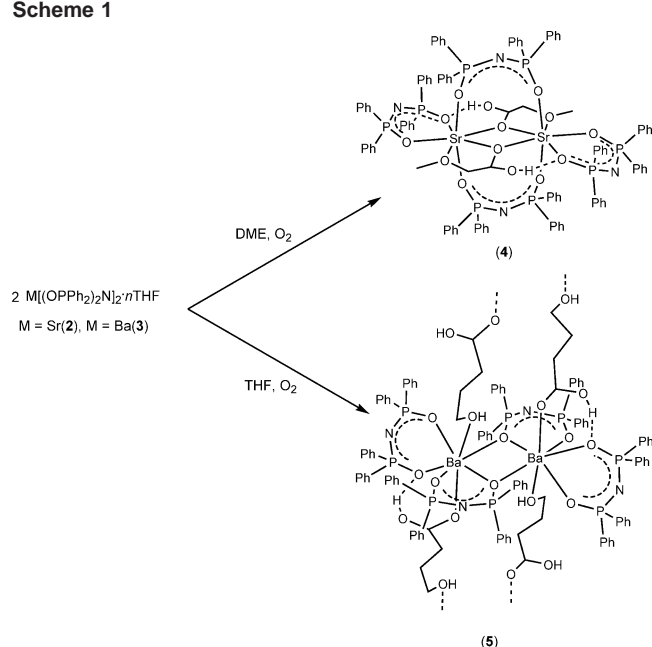
Attempts to grow X-ray-quality crystals of **2** and **3** from their DME and THF solutions, respectively, resulted in the oxidation of the coordinated solvent molecules. Thus, crystals of a dinuclear complex **4** were obtained from a DME solution of **2** upon storage at ambient temperature for several weeks.

\* To whom correspondence should be addressed. E-mail: cea@servidor.unam.mx.

- (1) Mijs, W. J.; De Jonge, C. R. H. I. *Organic Synthesis by Oxidation with Metal Complexes*; Plenum Press: New York, 1986.
- (2) Heyns, K.; Buchholz, H. *Chem. Ber.* **1976**, *109*, 3707–3727.
- (3) Reetz, M. T.; Töller, K. *Tetrahedron Lett.* **1995**, *36*, 9461–9464.
- (4) Li, P.; Alper, H. *J. Mol. Catal.* **1992**, 143–152.
- (5) Sommovigo, M.; Alper, H. *J. Mol. Catal.* **1994**, 151–158.
- (6) Bressan, M.; Morvillo, A.; Romanello, G. *J. Mol. Catal.* **1990**, *29*, 2976–2979.
- (7) Hirai, K.; Nutton, A.; Maitlis, P. M. *J. Mol. Catal.* **1981**, *10*, 203–211.
- (8) Straub, T.; Koskinen, A. M. P. *Inorg. Chem. Commun.* **2002**, *5*, 1052–1055.
- (9) Moreira, R. F.; Tshuva, E. Y.; Lippard, S. J. *Inorg. Chem.* **2004**, *43*, 4427–4434.

- (10) Morales-Juárez, J.; Cea-Olivares, R.; Moya-Cabrera, M.; García-Montalvo, V.; Toscano, R. A. *Main Group Chem.* **2005**, *4*, 23–31.
- (11) Kräuter, G.; Sunny, S. K.; Rees, W. S. *Polyhedron* **1998**, *17*, 391–395.
- (12) Haiduc, I.; Zukerman-Schpector, J.; Castellano, E.; Cea-Olivares, R. *Heteroat. Chem.* **2000**, *11*, 244–248.

Scheme 1



Similarly, **5** was isolated from a THF solution of **3** in a quantitative yield (Scheme 1). The coordination of methoxyacetic and  $\gamma$ -hydroxybutyric acids to the metal centers in **4** and **5**, respectively, clearly indicates an in situ oxidation of the solvents used for their crystallization. To gain further insight into this process, we followed the reaction using <sup>1</sup>H NMR spectroscopy. Periodic measurement of the <sup>1</sup>H NMR spectra of THF solutions of **2** and **3** under aerobic conditions revealed the presence of  $\alpha$ -hydroperoxytetrahydrofuran molecules after 1 week.<sup>13</sup> Thus, we confirmed the presence of  $\alpha$ -hydroperoxide as an intermediate in the oxidative degradation of these solvents.<sup>9</sup> It is noteworthy to mention that no evidence of an oxidation process was observed in the absence of air. Moreover, studies using BaCl<sub>2</sub> and SrCl<sub>2</sub> in THF under conditions similar to those mentioned above showed no significant formation of  $\alpha$ -hydroperoxytetrahydrofuran. Therefore, the oxidation behavior of **2** and **3** can be considered as a property of these complexes as a whole and not as an intrinsic property of the metal centers involved.

Compounds **4** and **5** exhibit spectroscopic patterns similar to those of their parent compounds **2** and **3**. Additionally, a peak at *m/z* 1941 assigned to the Ba<sub>2</sub>[(OPPh<sub>2</sub>)<sub>2</sub>N]<sub>4</sub> fragment of **5** revealed the dimeric nature of this compound, which was further confirmed by X-ray structural analysis. The crystal structures of **4** and **5** are illustrated in Figures 1 and 2, respectively.<sup>14</sup> Compounds **4** and **5** crystallize in a triclinic space group *P* $\bar{1}$  with half of the molecule in the asymmetric unit.

The centrosymmetric dinuclear complex **4** contains heptacoordinated strontium atoms in distorted pentagonal-bipyramidal geometry. The two P–N–P ligands are not equivalent; the first is chelating with both oxygen atoms attached to the same Sr atom (O1 and O2), whereas the second is bridging between the strontium atoms (O3 and O4).

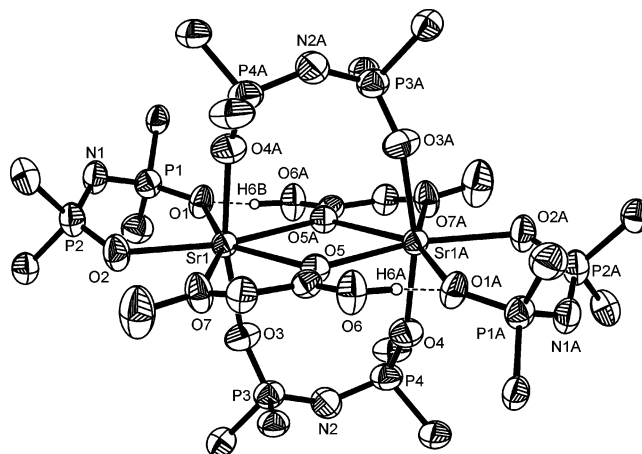


**Figure 1.** ORTEP representation (30% probability ellipsoids) of **4**. Carbon and hydrogen atoms of the phenyl groups (except C<sub>ipso</sub>) and hydrogens of the methoxyacetic acid (except the COOH proton) are omitted for clarity. Selected distances (Å) and bond angles (deg): Sr1–O4A, 2.396(2); Sr1–O3, 2.411(2); Sr1–O2, 2.475(2); Sr1–O1, 2.542(1); Sr1–O7, 2.603(2); Sr1–O5, 2.673(1); Sr1–O5A, 2.703(2); H6A⋯O1, 1.47(2); O3–Sr1–O4A, 167.1(1); O1–Sr1–O5A, 73.3(1); O2–Sr1–O1, 78.2(1); P1–N1–P2, 127.6(1); O2–Sr1–O7, 76.9(1); P3–N2–P4, 139.1(1); O6A–H6A⋯O1, 172(2).

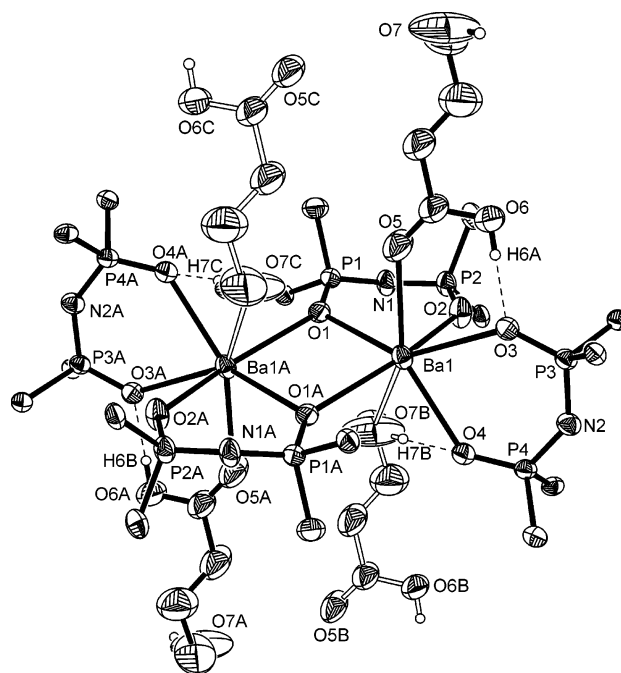


**Figure 2.** ORTEP representation (30% probability ellipsoids) of **5**. Carbon and hydrogen atoms of the phenyl groups (except C<sub>ipso</sub>) and hydrogens of the  $\gamma$ -hydroxybutyric acid (except OH) are omitted for clarity. The  $\gamma$ -hydroxybutyric acid molecules containing O7B and O7C are the symmetry equivalents of those containing O7A and O7B. Selected distances (Å) and bond angles (deg): Ba1–O2, 2.589(3); Ba1–O4, 2.682(3); Ba1–O3, 2.758(3); Ba1–O1A, 2.771(3); Ba1–O5, 2.773(5); Ba1–O5, 2.673(1); Ba1–O7B, 2.814(5); Ba1–O1, 2.837(3); H6A⋯O3, 1.73(2); H7⋯O4, 2.28(2); O1–Ba1–O1A, 81.3(1); O4–Ba1–O1A, 90.7(1); O2–Ba1–O1, 78.4(1); O5–Ba1–O7B, 149.4(2); O2–Ba1–O3, 75.0(1); P1–N1–P2, 132.8(3); O4–Ba1–O3, 74.2(1); P3–N2–P4, 137.2(3); O6–H6A⋯O3, 174(2); O7B–H7B⋯O4, 150(2).

The coordination sphere at each Sr atom is completed by the etheric oxygen atom (O7) and  $\mu^3$ -O of the carbonyl group (O5) belonging to two methoxyacetic acid molecules. The bridging coordination of the carbonyl group results in a planar Sr<sub>2</sub>O<sub>2</sub> core with a Sr⋯Sr distance of 4.370(2) Å.

(13) The reaction was followed by monitoring of the appearance of the C–H protons  $\alpha$  to the –OOH group ( $\delta$  5.52 ppm for **2** and 5.57 ppm for **3**).

Although there are no similar compounds for comparison, this Sr $\cdots$ Sr distance is within that observed for multinuclear strontium complexes containing Sr<sub>2</sub>O<sub>2</sub> units (3.425–4.564 Å).<sup>15</sup>

The five oxygen atoms (O1, O2, O5, O5A, and O7) of the bipyramidal base are nearly in the same plane (sum of the angles 360.1°), whereas the axial angle O3–Sr1–O4A is 167.1°. The Sr1–O4A (2.396(2) Å) and Sr1–O3 (2.411(2) Å) bond lengths corresponding to the bridging ligands are slightly shorter than those for the nonbridging Sr1–O bonds (average 2.509(2) Å). The P–N–P angles for the bridging ligands (139.1(1)°) are more obtuse than those for the nonbridging ligands (127.6(1)°). Similar to **4**, compound **5** is a dimeric centrosymmetric species with two heptacoordinated barium atoms displaying highly distorted pentagonal-bipyramidal environments (Figure 2). Two  $\mu^3$ -O atoms (O1 and O1A) from two equivalent molecules of the ligand bridge the barium atoms and form a planar Ba<sub>2</sub>O<sub>2</sub> core with a

Ba $\cdots$ Ba distance of 4.254(7) Å. The second oxygen atoms of these ligand molecules (O2 and O2A) coordinate each to one barium atom. Each barium atom is further coordinated to another molecule of the ligand (O3 and O4) and the oxygen atoms of the hydroxy (O7B) and carbonyl (O5) groups from two molecules of  $\gamma$ -hydroxybutyric acid. The equatorial sites around Ba1 are occupied by O1, O4, O5, O7B, and O3. The first four oxygen atoms and Ba1 are located within the same plane with a mean deviation of 0.049 Å, while O3 lies 0.969 Å out of the plane. The axial positions are occupied by O1A and O2, giving an axial angle of 155.6(1)°. In both compounds, the COOH and OH protons are involved in intramolecular hydrogen bonding. On the basis of the coordination environment of the barium, compound **5** is best described as a polymeric chain of inorganic cores linked by molecules of  $\gamma$ -hydroxybutyric acid and surrounded by phenyl groups.

In summary, the hitherto unknown imidodiphosphate complexes of group 2 metals represent a new class of entities capable of achieving oxidative degradation of cyclic and acyclic ethers. This noteworthy feature opens a new perspective for the application of group 2 metals. Further research is currently underway to determine the nature of this oxidative process.

**Acknowledgment.** V.J. thanks UNAM for his postdoctoral fellowship. We thank the Consejo Superior de Investigaciones Científicas of Spain for the license of the CSD.

**Supporting Information Available:** Experimental data of **2–5** and X-ray structural information in CIF format for **4** and **5**. This material is available free of charge via the Internet at <http://pubs.acs.org>.

IC050724H

- (14) Crystallographic data collection for **4**: C<sub>102</sub>H<sub>92</sub>N<sub>4</sub>O<sub>14</sub>P<sub>8</sub>Sr<sub>2</sub>, MW = 2020.80 g·mol<sup>-1</sup>, crystal 0.478 × 0.422 × 0.144 mm<sup>3</sup>, triclinic, space group *P*1, *a* = 13.760(1) Å, *b* = 14.015(1) Å, *c* = 14.379(1) Å,  $\alpha$  = 81.482(1)°,  $\beta$  = 65.576(2)°,  $\gamma$  = 82.575(1)°, *V* = 2489.8(3) Å<sup>3</sup>, *Z* = 1, *T* = 293(2) K, *R*1 = 0.0559 for *I* > 2 $\sigma$ (*I*), *wR*2 = 0.0746 for all data. Crystallographic data collection for **5**: C<sub>104</sub>H<sub>96</sub>Ba<sub>2</sub>N<sub>4</sub>O<sub>14</sub>P<sub>8</sub>, MW = 2148.29 g·mol<sup>-1</sup>, crystal size 0.196 × 0.144 × 0.110 mm<sup>3</sup>, triclinic, space group *P*1, *a* = 10.678(1) Å, *b* = 14.646(1) Å, *c* = 18.326(1) Å,  $\alpha$  = 109.106(2)°,  $\beta$  = 98.516(2)°,  $\gamma$  = 106.300(1)°, *V* = 2506.6(3) Å<sup>3</sup>, *Z* = 1, *T* = 293(2) K, *R*1 = 0.0591 for *I* > 2 $\sigma$ (*I*), *wR*2 = 0.1309 for all data. For further details, see the Supporting Information.
- (15) For some of the shortest (a–c) and longest (d–f) Sr $\cdots$ Sr distances within a Sr<sub>2</sub>O<sub>2</sub> unit, see: (a) Baxter, I. A.; Darr, J. A.; Drake, S. R.; Hursthouse, M. B.; Malik, K. M. A.; Mingos, D. M. P. *J. Chem. Crystallogr.* **1998**, *28*, 221–226. (b) Deacon, G. B.; Forsyth, C. M.; Junk, P. C. *J. Organomet. Chem.* **2000**, *607*, 112–119. (c) Baxter, I. A.; Darr, J. A.; Drake, S. R.; Hursthouse, M. B.; Malik, K. M. A.; Mingos, D. M. P. *J. Chem. Soc., Dalton Trans.* **1997**, 2875–2885. (d) Hundal, G.; Hundal, M. S.; Singh, N. *J. Chem. Crystallogr.* **2004**, *34*, 447–451. (e) Insausti, M.; Urriaga, M. K.; Cortes, R.; Mesa, J. L.; Arriortua, M. I.; Rojo, T. *J. Mater. Chem.* **1994**, *4*, 1867–1870. (f) Gil de Muro, I.; Insausti, M.; Lezama, L.; Pizarro, J. L.; Arriortua, M. I.; Rojo, T. *Eur. J. Inorg. Chem.* **1999**, 935–943.